



 Cite this: *RSC Adv.*, 2023, **13**, 34916

# Quantifying arsenic and mercury in aqueous media via bio-inspired gold nanoparticles modified by mango leaf extract†

 Bijoy Sankar Boruah,<sup>a</sup> Rajib Biswas <sup>\*b</sup> and Nirmal Mazumder<sup>\*c</sup>

The present study conveys a new method for detecting arsenic(III) and mercury(II) in aqueous solution via bio-inspired gold nanoparticles. The process of synthesizing gold nanoparticles involves the utilization of the chemical reduction method. The functionalization of gold nanoparticles' surface is achieved via mango leaf extract. The as-synthesized nanoparticles are characterized by UV-Vis and DLS which reveal a plasmonic peak around ~520 nm with an average size distribution of ~44 nm. The modified gold nanoparticles have demonstrated selective detection capabilities towards arsenic(III) as well as mercury(II), as evidenced by color changes observed in the presence of ions of arsenic as well as mercury. The addition of mercury and arsenic lead to the overall aggregation—thereby bringing a colorimetric response. The limit of detection was determined to be 1 ppb and 1.5 ppb for arsenic(III) and mercury(II) ions, respectively along with exceptional linearity.

 Received 26th October 2023  
 Accepted 22nd November 2023

DOI: 10.1039/d3ra07293b

[rsc.li/rsc-advances](https://rsc.li/rsc-advances)

## 1. Introduction

Heavy metal ions in water are toxic and pose a serious issue for the environment and human health. Consuming water that contains metal ions can cause a variety of health problems. Mercury, lead, nickel, copper, and arsenic are heavy metal ions that are frequently found in water.<sup>1–5</sup> Since they are a component of Earth's crust, these metal ions are ubiquitous. Water pollution is mostly caused by anthropogenic sources, such as the industrial and agricultural use of metal compounds. The most dangerous and harmful ions are mercury(II) and arsenic(III), whose consumption can lead to a variety of health issues, including brain damage, kidney failure, skin cancer, nervous system issues, *etc.*<sup>6–8</sup> Mercury and arsenic concentrations in water are permitted to be no more than 6 ppb and 10 ppb, respectively as per the World Health Organization's guidelines.<sup>8–10</sup> Monitoring metal ions in water has become a difficult task for the scientific community because of the increased application of heavy metal ions in industrial domains.<sup>11–13</sup> There are numerous methods, including atomic absorption spectrometry, atomic fluorescence spectrometry, and inductively coupled plasma mass spectrometry, to find

metal ions in water. These methods have the drawback of being intricate, time-consuming, and expensive.<sup>13–15</sup>

The use of nanoparticles for heavy metal monitoring has recently received a lot of attention.<sup>11,12</sup> Due to their size, shape, interparticle spacing, and external dielectric environment, nanoparticles differ greatly from their bulk counterparts. Nanoparticles' special physical, chemical, and electrical characteristics have applications in the realm of sensing. Since the colorimetric method is straightforward, affordable, and visible to the naked eye, many research projects have been reported to detect heavy metal ions using this methodology. They have been utilized as sensing units because of the special optical features of gold and silver nanoparticles. For the detection of arsenic(III) using a colorimetric method, functionalized gold nanoparticles, S-layer functionalized gold nanoparticles, aptamer and gold nanoparticles, aptamer conjugated silver nanoparticles, and citrate capped gold nanoparticles have all been described.<sup>5–7</sup> Meanwhile, colorimetric detection of mercury(II) utilizing silver and gold nanoparticles has also been reported.<sup>10–12</sup> It has been shown that most of the investigators used the chemical reduction method to create nanoparticles, which involves the use of rigorous chemical reagents such as sodium borohydride or trisodium citrate. Since these nanoparticles are hazardous, they pollute the environment after their use.<sup>13–15</sup>

On the contrary, green nanotechnology is a method of creating environment friendly nanoparticles by synthesizing them using green reagents. Green reagents have several benefits because they are ecofriendly, biocompatible, and biodegradable.<sup>16–18</sup> One of the most popular green technologies is the synthesis of nanoparticles using plant leaf extract owing to presence of antioxidant compounds in some leaf extracts,

<sup>a</sup>Department of Physics, Rangapara College, Rangapara, Assam, India

<sup>b</sup>Department of Physics, Applied Optics and Photonics Research Laboratory, Tezpur University, Tezpur-784028, India. E-mail: rajib@tezu.ernet.in

<sup>c</sup>Department of Biophysics, Manipal School of Life Sciences, Manipal Academy of Higher Education, Manipal, Karnataka, India-576104. E-mail: nirmal.mazumder@manipal.edu

 † Electronic supplementary information (ESI) available. See DOI: <https://doi.org/10.1039/d3ra07293b>


which can reduce silver or gold.<sup>19,20</sup> *Hibiscus rosa-sinensis*, neem, tulsi, and other plant leaf extracts, among others, have a few biomedical uses and can be used to create nanoparticles.<sup>20,21</sup> Using a composite of graphene oxide and silver nanoparticles to detect arsenic(III), which uses green reagents such as ascorbic acid as a reducing agent and beta-cyclodextrin as a stabilizer, silver nanoparticles for mercury(II) detection, L-tyrosine stabilized silver and gold nanoparticles for mercury, lead, and magnesium detection, and magnesium, lead, and lead nanoparticles have all been reported based on green synthesis using papaya fruit extract, which is found to be very helpful to detect heavy metal ions.<sup>18–23</sup>

The goal of this work is to develop environmentally benign methods for making metal nanoparticles that are low in toxicity, biocompatible, biodegradable, and have uses in environmental monitoring. *Mangifera indica* leaf (mango leaf) extract was employed in this instance to functionalize the gold nanoparticles.<sup>11,12</sup> The chemical composition of mango leaf extract can vary depending on factors such as growing conditions, and the extraction method used. However, mango leaf extract typically contains a variety of phytochemicals [see S1 of ESI†], including polyphenols, terpenoids, sterols *etc.* They are widely used in functionalizing nanoparticles for various application domain such as sensing, catalytic activity *etc.*<sup>12–14</sup> Inspired by these, herein, we exhibit simultaneous detection of mercury(II) and arsenic(III) *via* modified gold nanoparticles made from mango leaf extract. Chitosan, a biodegradable biopolymer, is used as a reducing agent in the manufacture of gold nanoparticles.<sup>5–11</sup> These environmentally benign, biochemically mediated gold nanoparticles can be utilized to find heavy metals in aqueous medium.

## 2. Experimental section

### 2.1. Materials and chemicals

Gold chloride and chitosan of medium weight were purchased from Sigma-Aldrich to make gold nanoparticles (U.S.A). Merck provided metal salts like sodium arsenite, copper chloride, lead chloride, nickel chloride, cadmium chloride, mercury chloride, and nickel chloride (U.S.A). All glassware are cleaned using aqua regia solution. All required solutions are prepared using double distilled water. Mango leaves were gathered from Tezpur University campus.

### 2.2. Instrumentations

The optical characteristics of green synthesis gold nanoparticles are examined *via* UV-vis spectrometer (UV-2450, Shimadzu). The pH of gold nanoparticles is determined using a pH meter (Eco tester pH1, Eutech Instruments). Dynamic light scattering was used to observe the distribution of nanoparticle sizes (DLS, Nanoplus-3).

### 2.3. Green synthesis of gold nanoparticles

To make the gold nanoparticles used in this study environmentally benign, we used a green method of synthesis. A 3-weight percent chitosan solution is made in 0.2 M of acetic acid

at room temperature, followed by 8 hours of stirring, before making the gold chloride solution. 100 ml of a 1 mM gold chloride solution are taken, put in a conical flask, and heated on a magnetic stirrer till boiling. 5 ml gold chloride solution is then added to the chitosan solution. After a few minutes, it is seen that the solution has changed to the color of red wine—signifying the formation of gold nanoparticles. These nanoparticles are maintained at 40 °C for subsequent use after being cooled to ambient temperature.

### 2.4. Modification of gold nanoparticles

We have modified the as-prepared gold nanoparticles with a green substance for use in the detection of metal ions that pollute water. This emerald substance is an extract from the mango leaf. The mango leaf is washed under running water, then repeatedly rinsed with double-distilled water while being held at room temperature for 30 minutes. 10 grammes of these leaves are gathered and chopped into little pieces. These leaf pieces are cooked for 15 minutes at 600 °C in 100 cm<sup>3</sup> of purified water. We have filtered these solutions *via* Whatman filter paper after cooling. Mango leaf extract solution appears to be having a pale-yellow tint in the solution. This solution is then maintained at 40 °C for subsequent use.

We have taken 6 ml of gold nanoparticles and placed them in a centrifuge tube for alteration. 3 ml of *Mangifera* leaf extract is added to this nanoparticle solution and allowed to settle for a little while. *Via* a UV-vis spectrometer, the optical response of these modified nanoparticles is analyzed which shows its characteristic surface plasmon resonance peak [SPR].

## 3. Results and discussions

### 3.1. Selectivity of ions

Here, we've used gold nanoparticles made from green synthesis to detect ions in water. Fig. 1(a) and (b) illustrate, respectively, the optical response of gold nanoparticles and modified gold nanoparticles together with the size distribution of the particles. Fig. 1(a) shows that the peak of the surface plasmon resonance occurs at a wavelength of 524 nm, suggesting that nanoparticles are spherical. The absorption value of modified gold nanoparticles is higher than that of unmodified gold nanoparticles, giving them a pronounced peak. This indicates that the surface of the gold nanoparticles was changed and stabilized by the mango leaf extract. Fig. 1(b) displays the particle size distribution of modified gold nanoparticles. It is found that the modified gold nanoparticles have an average particle size ~44 nm. 0.5 ml of pristine gold nanoparticle solutions are taken in some centrifuge tubes for detecting metal ions. Gold nanoparticles modified by leaf extract are also taken in separate tubes. These tubes are filled with various ions solutions, including those containing copper, arsenic, lead, mercury, nickel, and cadmium, respectively. It has been noted that centrifuges holding pristine gold nanoparticles did not exhibit any color change upon the addition of ions solutions. This implies that pristine nanoparticles are incapable of identifying the ions. Nevertheless, gold nanoparticles treated with



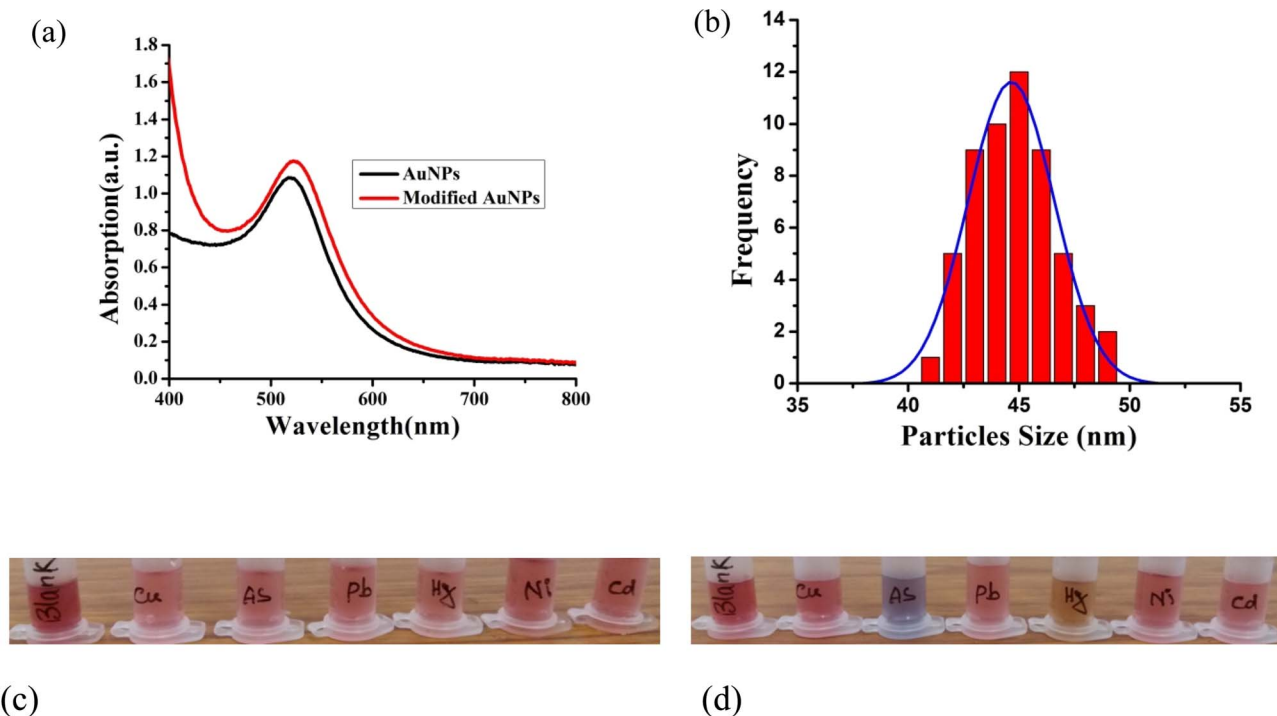


Fig. 1 (a) UV-Vis spectra of pristine and modified AuNPs, (b) size distribution of AuNPs, colorimetric response of (c) pristine AuNPs and (d) modified AuNPs.

mango leaf extract have displayed an excellent color change in arsenic and mercury-containing tubes. This suggests that these modified gold nanoparticles may be used to colorimetrically detect arsenic(III) and mercury(II) in water.

### 3.2. UV-vis response of metal ions containing modified gold nanoparticles

We performed a UV-vis spectrometry test to confirm the modified gold nanoparticles' selectivity towards heavy metal ions.

The optical response and distinctive SPR peak of metal ions containing gold nanoparticles are depicted in Fig. 2(a). Arsenic(III) and mercury(II)-containing gold nanoparticles are seen to have altered SPR peaks relative to the others. In case of arsenic, there is a red shift characterized by two peaks at 530 nm and 612 nm. In most cases, an increase in the refractive index of the surrounding medium leads to a redshift of the SPR peak. This means that the resonance wavelength of the gold nanoparticles becomes longer (moves toward the red end of the spectrum)

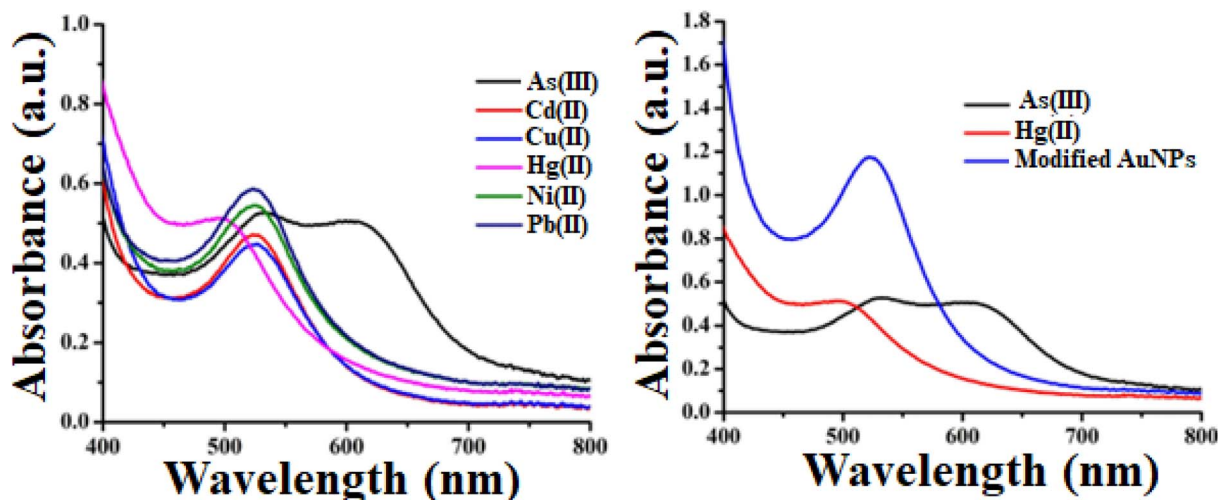


Fig. 2 (a) Optical response and distinctive SPR peak of metal ions containing gold nanoparticles, (b) SPR peaks of As, Hg and modified AuNPs [added concentration of heavy metal ions is 3 ppb].



after the addition of arsenic(III). This redshift is a characteristic response of plasmonic nanoparticles to changes in the local environment. On the contrary, mercury has a blue shift with a peak at 490 nm. Fig. 2(b) makes it very evident how the SPR peak, upon addition of arsenic(III) and mercury(II) solution, shifted from the modified gold nanoparticles peak. The mechanism of SPR peak shift and color change is described in section 3.3.

The blue-shift of the surface plasmon resonance (SPR) peak of gold nanoparticles upon the addition of mercury(II) is an interesting phenomenon that can be attributed to changes in the local refractive index and the electronic properties of the gold nanoparticles. When gold nanoparticles are dispersed in a solution, the SPR peak is highly sensitive to changes in the refractive index of the surrounding medium. The SPR peak is typically observed in the visible region of the electromagnetic spectrum. Owing to addition of mercury(II) ions to the solution containing gold nanoparticles, the refractive index of the medium around the nanoparticles changes. This change in refractive index leads to a shift in the SPR peak.

### 3.3. Mechanism of color change

In our study, we employed mango leaf extract to modify green synthesized gold nanoparticles for colorimetric detection of heavy metal ions in aqueous medium. From the illustration, it is evident that heavy metal ions do not significantly alter the hue of pristine gold nanoparticles. This shows that these pristine gold nanoparticles lack the ability to selectively detect metal ions. However, the color alteration in arsenic(III) and mercury(II)-containing tubes is quite prominent, as illustrated in Fig. 2(a). Arsenic- and mercury-added tubes displayed bluish and brown colors, respectively. Fig. 2(b) shows the distinct variation in absorbance of modified AuNPs *via* mango leaf extract in presence of As(III) and Hg(II). This suggests that

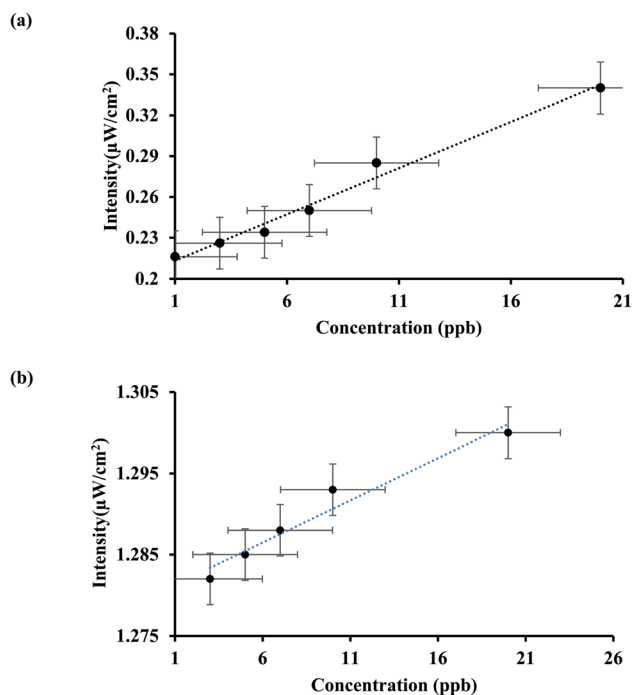


Fig. 4 (a) Intensity vs. concentration plot for mercury(II); (b) intensity vs. concentration plot for arsenic(III).

modified gold nanoparticles *via* mango leaf extract are capable of detecting arsenic and mercury in aqueous medium. Fig. 3 depicts the mechanism by which modified gold nanoparticles interact with arsenic and mercury (b). Fig. 3(a) illustrates the manufacturing and modification procedure of gold nanoparticles. Fig. 3(b) suggests the binding mechanism of arsenic and mercury with modified gold nanoparticles for which color change is noticed.

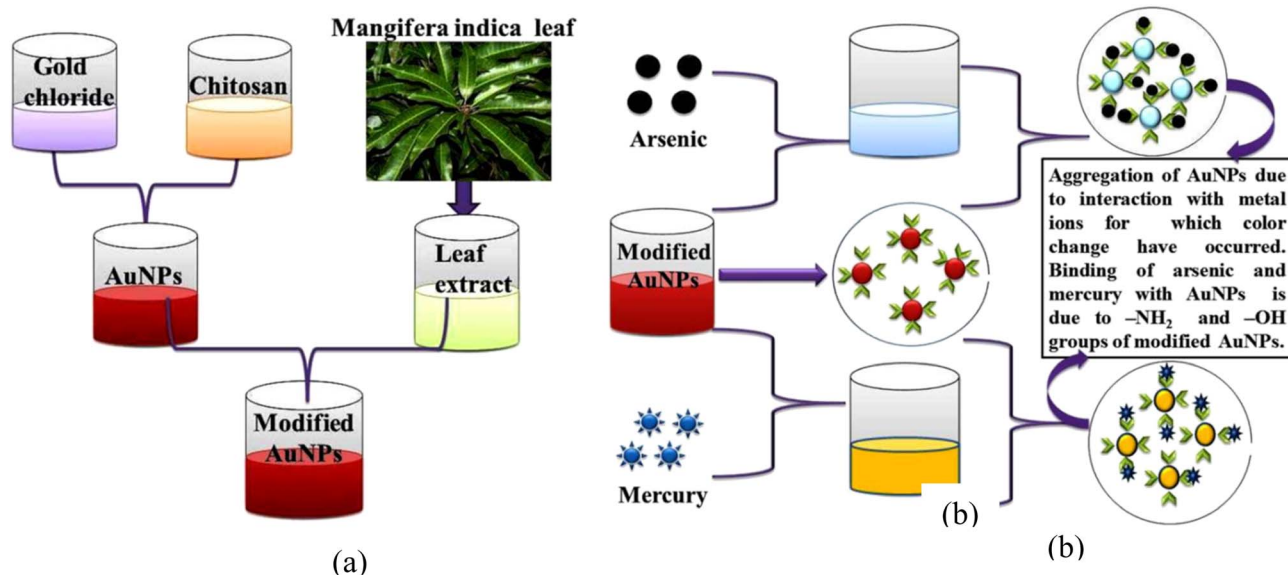


Fig. 3 (a) Schematic representation of modification of AuNPs *via* mango leaf extract, (b) mechanism of colorimetric response with respect to arsenic(III) and mercury(II).



It is generally known that nanoparticles display various colors because of surface plasmon resonance (SPR) characteristics. The form, size, and interparticle distance of nanoparticles all affect their SPR characteristics. Mango leaf extract contains several biomolecules, including thiamine, terpenoids, and flavonoids. These biomolecules include a hydroxyl group ( $-OH$ ) and an amino group ( $-NH_2$ ). As reported by several research groups,<sup>9–11</sup> amino and hydroxyl groups can bind to mercury and arsenic. Modification of gold nanoparticles *via* mango leaf extract introduces amino and hydroxyl groups to their surfaces. Upon addition of mercury(II) and arsenic(III) ions, the modified nanoparticles bind these metal ions with amino and hydroxyl groups. The modification of nanoparticles with *Mangifera indica* extracts might alter the surface characteristics of the nanoparticles, making them more selective towards mercury and arsenic ions. This selective binding can facilitate the detection process. Apart from this, arsenic and mercury possess different electron affinities. In addition, they are Lewis acids leading to varying extent of Lewis acid–base reactions with modified gold nanoparticles.<sup>10–12</sup> As a result, the possibility of interference remains minimal. Meanwhile, the inter-particle spacing between the nanoparticles decreases because of mercury and arsenic interaction with nanoparticles—thereby leading to aggregation of the nanoparticles to different extents. Consequently, the color of the gold nanoparticles changes throughout this aggregation process from wine red to brown and bluish for mercury(II) and arsenic(III), respectively which is confirmed by the UV-Vis spectra as given Fig. 2. Thus, selective binding can facilitate the overall detection process.

We then proceed to compute the limit of detection of mercury(II). Fig. 4(a) demonstrates the satisfactory rising and linear intensity profile for mercury with increasing concentration. It turns out that the obtained linearity is consistent within a considerable concentration range of 1 to 20 ppb along with a regression value of  $\sim 0.99$ . Following,<sup>6–11</sup> the limit of detection is found to be 1.5 ppb using the formula  $3\sigma/m$  where  $\sigma$  and  $m$  correspond to standard error and slope of linear fit, respectively. Likewise, we did estimate the sensing attributes for arsenic(III) ion. The bioinspired AuNPs yields an excellent performance for arsenic(III) ion too. As evident in Fig. 4(b), the regression value emerges to be  $\sim 0.98$ . Likewise, the limit of detection is found to be 1 ppb.

In addition to these studies, we tested the setup using real samples. We examined the tap water. The tap water samples have been contaminated with As and Hg ions in concentrations of 5, 7, and 10 ppb without any form of pre-treatment. It has been found that these spiked samples, when conjugated with the as-modified AuNPs, yielded values which are in proximity with the actual values. The recovery efficacies as per this colorimetric probe stand at  $\sim 96\%$  for both mercury(II) and arsenic(III) [see attached ESI S2; T1 & T2†].

Further, a comparative analysis of this work has been performed with other reported works [see T3 of ESI†]. As can be seen, the LOD of our work is comparatively better in comparison to others. Likewise, most of the reported works utilized chemically modified gold nanoparticles. In our study, we stick to benign route by utilizing mango leaf extract for

functionalizing the gold nanoparticles. Another notable feature of this work is the dual sensing of two pervasive metal ion with a remarkable limit of detection and recovery efficiency.

## 4. Conclusion

Overall, bioinspired AuNPs have been synthesized *via* benign route where mango leaf extract has been utilized for functionalization. The modified AuNPs have been then subjected to added concentration of mercury(II) and arsenic(III). It has been observed that the colorimetric sensing scheme aided by mango leaf extract has been performing nicely with good repeatability. The linearity indices for both arsenic and mercury emerge to be unity. Further, the recovery tests conducted with tap water are found to be yielding a remarkable retrieval efficiency of  $\sim 96\%$ .

## Conflicts of interest

Authors declare no competing interest.

## Acknowledgements

The support received from DST-FIST and UGC-SAP DRSII grant-in-aid to the Department of Physics is thankfully acknowledged.

## References

- 1 A. K. Tareen, I. N. Sultan, P. Parakulsuksatid, M. Shafi, A. Khan, M. W. Khan and S. Hussain, *Int. J. Curr. Microbiol. Appl. Sci.*, 2014, **3**(1), 299–308.
- 2 S. H. Choi, *et al.*, *Anal. Lett.*, 2019, **52**(3), 496–510.
- 3 A. Ono and H. Togashi, *Angew. Chem.*, 2004, **116**(33), 4400–4402.
- 4 Y. Kim, R. C. Johnson and J. T. Hupp, *Nano Lett.*, 2001, **1**, 165–167.
- 5 D. W. Kimmel, G. LeBlanc, M. E. Meschievitz and D. E. Cliffel, *Anal. Chem.*, 2012, **84**, 685–707.
- 6 R. Biswas, C. Barman, A. Neog, S. Biswas and N. Mazumder, *Chemosphere*, 2023, **322**, 138231.
- 7 M. Li, H. Gou, I. Al-Ogaidi and N. Wu, *ACS Sustainable Chem. Eng.*, 2013, 713–723.
- 8 S. Biswas and R. Biswas, *Chemosphere*, 2023, **312**, 137187.
- 9 R. Biswas, R. Bhuyan, B. S. Boruah and N. Mazumder, *Opt. Fiber Technol.*, 2022, **72**, 102996.
- 10 B. S. Boruah and R. Biswas, *Opt. Laser Technol.*, 2021, **137**, 106813.
- 11 B. S. Boruah and R. Biswas, *IEEE Sens. Lett.*, 2019, **3**(3), DOI: [10.1109/LESENS.2019.2894419](https://doi.org/10.1109/LESENS.2019.2894419).
- 12 B. S. Boruah, R. Biswas and N. Ojah, *J. Lightwave Technol.*, 2020, **38**(7), 2086–2091.
- 13 Y. Cai, J. Zhang, M. Zhang, M. Wang and Y. Zhao, *Sens. Actuators, B*, 2022, **364**, 31857.
- 14 B. S. Boruah, R. Biswas and U. Neog, *Plasmonics*, 2021, **15**, 1903–1912.
- 15 S. Gao, *et al.*, *Anal. Chem.*, 2009, **81**(18), 7703–7712.
- 16 B. D. Gupta, H. Dodeja and K. Tomar, *Opt. Quantum Electron.*, 1996, **28**, 1629–1639.



## Paper

- 17 J. S. Lee, M. S. Han and C. A. Mirkin, *Angew. Chem.*, 2007, **119**(22), 4171–4174.
- 18 Y. Long, H. Li, W. Wang, X. Yang and Z. Liu, *J. Alloys Compd.*, 2022, **910**, 164916.
- 19 D. Paul and R. Biswas, *Environ. Technol. Innovation*, 2022, **25**, 102112.
- 20 G. M. Shukla, N. Punjabi, T. Kundu and S. Mukherji, *IEEE Sens. J.*, 2019, **19**(9), 3224–3231.
- 21 T. Shtoyko, A. T. Maghasi, J. N. Richardson, C. J. Seliskar and W. R. Heineman, *Anal. Chem.*, 2004, **76**(5), 1466–1473.
- 22 X. H. Zhao, R. M. Kong, X. B. Zhang, H. M. Meng, W. N. Liu, W. Tan, G. L. Shen and R. Q. Yu, *Anal. Chem.*, 2011, **83**(13), 5062–5066.
- 23 *Environmental Contamination: Health Risks and Ecological Restoration*, ed. M. H. Wong, CRC Press, 1st edn, 2012, DOI: [10.1201/b12531](https://doi.org/10.1201/b12531).

